

Video Article

Fiber Connections of the Supplementary Motor Area Revisited: Methodology of Fiber Dissection, DTI, and Three Dimensional Documentation

Baran Bozkurt¹, Kaan Yagmurlu², Erik H. Middlebrooks³, Zuzan Cayci⁴, Orhun M. Cevik¹, Ali Karadag⁵, Sean Moen¹, Necmettin Tanriover⁶, Andrew W. Grande¹

¹Department of Neurosurgery, University of Minnesota

²Department of Neurosurgery, Barrow Neurological Institute, St. Josephs Hospital and Medical Center

³Department of Radiology, University of Alabama at Birmingham

⁴Department of Radiology, University of Minnesota

⁵Department of Neurosurgery, Tepecik Training and Research Hospital

⁶Department of Neurosurgery, Cerrahpasa Medical School, University of Istanbul

Correspondence to: Baran Bozkurt at bbozkurt@umn.edu

URL: <https://www.jove.com/video/55681>

DOI: [doi:10.3791/55681](https://doi.org/10.3791/55681)

Keywords: Neuroscience, Issue 123, Supplementary motor area, fiber dissection, diffusion tensor tractography, three-dimensional documentation, white matter pathways, association fibers, commissural fibers, projection fibers

Date Published: 5/23/2017

Citation: Bozkurt, B., Yagmurlu, K., Middlebrooks, E.H., Cayci, Z., Cevik, O.M., Karadag, A., Moen, S., Tanriover, N., Grande, A.W. Fiber Connections of the Supplementary Motor Area Revisited: Methodology of Fiber Dissection, DTI, and Three Dimensional Documentation. *J. Vis. Exp.* (123), e55681, doi:10.3791/55681 (2017).

Abstract

The purpose of this study is to show the methodology for the examination of the white matter connections of the supplementary motor area (SMA) complex (pre-SMA and SMA proper) using a combination of fiber dissection techniques on cadaveric specimens and magnetic resonance (MR) tractography. The protocol will also describe the procedure for a white matter dissection of a human brain, diffusion tensor tractography imaging, and three-dimensional documentation. The fiber dissections on human brains and the 3D documentation were performed at the University of Minnesota, Microsurgery and Neuroanatomy Laboratory, Department of Neurosurgery. Five postmortem human brain specimens and two whole heads were prepared in accordance with Klingler's method. Brain hemispheres were dissected step by step from lateral to medial and medial to lateral under an operating microscope, and 3D images were captured at every stage. All dissection results were supported by diffusion tensor imaging. Investigations on the connections in line with Meynert's fiber tract classification, including association fibers (short, superior longitudinal fasciculus I and frontal aslant tracts), projection fibers (corticospinal, claustricocortical, cingulum, and frontostriatal tracts), and commissural fibers (callosal fibers) were also conducted.

Video Link

The video component of this article can be found at <https://www.jove.com/video/55681/>

Introduction

Among the 14 frontal areas delineated by Brodmann, the premotor and prefrontal area that lies in front of the precentral motor cortex has long been considered as a silent module, despite the fact that the frontal lobe plays an important role in cognition, behavior, learning, and speech processing. In addition to the supplementary motor area (SMA) complex, consisting of the pre-SMA and the SMA proper (Brodmann Area; BA 6) that extends medially, the pre-motor/frontal module includes the dorsolateral prefrontal (BA 46, 8, and 9), frontopolar (BA 10), and ventrolateral prefrontal (BA 47) cortices, as well as part of the orbitofrontal cortex (BA 11) on the lateral surface of the brain^{1,2}.

The SMA complex is a significant anatomical area that is defined by its functions and its connections. The resection and damage of this region causes significant clinical deficits known as the SMA syndrome. The SMA syndrome is an important clinical condition that is particularly observed in frontal glioma cases that contain the SMA complex³. The SMA complex has connections with the limbic system, basal ganglia, cerebellum, thalamus, contralateral SMA, superior parietal lobe, and portions of the frontal lobes via fiber tracts. The clinical effect of damage to these white matter connections may be more severe than to the cortex. This is because the consequences of injury to the cortex can be ameliorated over time due to high cortical plasticity^{4,5,6,7,8,9,10,11,12}. Therefore, the SMA regional anatomy and the white matter pathways should be deeply understood, in particular for glioma surgery.

A comprehensive understanding of the anatomy of white matter pathways is important for the wide-spectrum treatment of neurosurgical lesions. Recent studies of the three-dimensional documentation of the anatomical results that were obtained in microsurgery were used to gain a better understanding of the topographical anatomy and the interrelationship of brain white matter pathways^{13,14}. Therefore, the purpose of this study was to examine the white matter connections of the SMA complex (pre-SMA and SMA proper) using a combination of fiber dissection techniques

on cadaveric specimens and magnetic resonance imaging (MRI) tractography and to explain all the methods and principles of both techniques and their detailed documentation.

Planning and Strategy of Study

Prior to performing the experiments, a literature search on the basic principles of fiber dissections, the procedures that need to be applied to specimens before and during dissections, and all connections between SMA regions that have been revealed with dissection and DTI was conducted. The previous studies on the anatomical localization and separation of pre-SMA and SMA-proper regions and on the topographic anatomy of their connections were reviewed.

Protocol

The deceased are included here as a population, although deceased persons are not technically human subjects; human subjects are defined by 45 CF 46 as "living human beings"^{15,16}.

1. Preparation of Specimens

1. Examine 5 formalin-fixed brains (10 hemispheres) and 2 whole human heads.
2. Fix the specimens in a 10% formalin solution for at least 2 months according to Klingler's method¹⁷.
3. Freeze all specimens at -16 °C for 2 weeks in accordance with Klingler's method¹⁷.
4. Thaw the specimens under tap water.
5. **Perform an extended frontotemporal craniotomy on the cadaveric head to expose the brain.**
 1. Place the cadaveric head in a three-pin skull clamp (**Material Table**).
 2. Make a frontotemporal skin incision with a scalpel.
 3. Remove the skin and muscles using a scalpel, forceps, and scissors.
 4. Make one or more burr holes in the skull until the dura mater is reached; use a drill with a compact speed reducer and a 14 mm cranial perforator attachment at 79,000 rpm (**Material Table**).
 5. Cut the bone flap and open the skull using a 2 mm x 15.6 mm fluted router with a 2.1 mm pin-shaped burr attachment at a drill speed of 80,000 rpm (**Material Table**).
6. Remove the dura, arachnoid, and pia mater and dissect using a microdissector under a microscope at 6X to 40X magnification^{5,18} (**Material Table**).

2. Fiber Dissection Technique

NOTE: Perform all dissections under 6X to 40X magnification on a surgical microscope.

1. **Perform the fiber dissections in a stepwise manner on each hemisphere, from lateral to medial and medial to lateral.**
 1. Decorticate the cerebral cortex using a panfield dissector (**Material Table**) and remove all frontal cortical tissues to expose the short association fiber tracts, which are U-fibers or intergyral fibers that interconnect neighboring gyri^{5,13}.
 2. Remove the short association fibers with a panfield dissector and a surgical micro hook by gently trimming under the microscope (**Material Table**) to reach and expose the long association fibers, which interconnect distant areas in the same hemisphere.
 3. Go deep into the long association fibers to remove the superficial association fibers using a surgical micro hook and a panfield dissector; remove each fiber bundle under a microscope (**Material Table**) to expose the projection commissural fibers.
 4. View each of the connections of the SMA complex according to the topographical anatomy that was previously defined in the literature^{2,8,18,19,20,21}.
2. Keep all specimens (whole heads and brains) that were used during the dissections in 10% formaldehyde solution (**Material Table**) between the dissection periods.

3. 3D Photography Technique

1. Use a black color platform during the photography of the specimens.
2. **Follow a 3D photography technique²².**
 1. Place each specimen in a designed black color platform.
 2. Select a scene with a full-frontal view of the specimen and take one shot by focusing the camera on any point on the specimen close to the center point on the camera screen (instrument table). Use an 18- to 55-mm f/3.5-5.6 SLR lens or a 100 mm f/2.8L macro lens and set the aperture to F29, ISO 100.
 3. Rotate the camera slightly left until the right-most point on the camera screen is the same as the focusing point above. Slide the camera to the right until the middle point on the screen overlaps the original focusing point on the specimen. Focus the camera on this point and take another shot.
 4. Maintain the distance and axis of the camera to the specimen being photographed at constant values.
3. **Create a 3D image by using a 3D image generator program (Material Table).**
 1. Open the 3D software program.
 2. Choose "Open stereo images from File."
 3. Select the two images (left and right) and make sure the left image is in the left slot and the right image is in the right slot.

4. Select the "Half color anaglyph RL/2" option and generate the anaglyph in jpeg format.

4. DTI Technique

1. Acquire pre-processed diffusion data utilizing the Human Connectome Project diffusion data²³ by downloading it from the referenced website. NOTE: The data is downloaded pre-processed and consisted of the following procedures: The diffusion data was acquired in normal volunteers using a modified 3 T MRI device (instrument table) utilizing a spin-echo echo planar imaging (EPI) sequence with multi-band image acceleration^{24,25,26,27,28}. Relevant sequence parameters include: TR = 5,520 ms; TE = 89.5 ms; FOV = 210 x 180 mm; matrix = 168 x 144; slice thickness = 1.25 mm (voxel size 1.25 x 1.25 x 1.25 mm); multiband factor = 3; and b-values = 1,000 s/mm² (95 directions), 2,000 s/mm² (96 directions), and 3,000 s/mm² (97 directions). The data was then processed utilizing FreeSurfer²⁹ and FSL³⁰; the process included eddy current correction, motion correction, b0 intensity normalization, susceptibility distortion correction, and gradient-nonlinearity correction^{28,31,32,33}. Corresponding T1-weighted MP-RAGE images are also included in the download package. Procedures are documented in the Human Connectome Project procedures manual²³.
2. **Post-process the diffusion data using Diffusion Spectrum Imaging (DSI) Studio³⁴ to generate an estimated voxel-wise diffusion orientation distribution function (ODF) employing a generalized q-sampling imaging (GQI) algorithm³⁵.**
 1. Load the downloaded dataset into the software by selecting "STEP1: Open source images" and selecting the data.nii.gz file.
 2. Select the "STEP2: Reconstruction" button. After verifying the brain mask, proceed to "Step 2" and select "GQI" as the reconstruction method. Select "r² weighting" with a "length ratio" of "1.0." Leave the remaining selections as the default.
 3. Select "Run reconstruction."
3. **Place appropriate seeds for regions-of-interest to streamline fiber-tracking.**
 1. In the "Region Window," click the "Atlas" button to place seeds for the superior longitudinal fasciculus (SLF) I. Select "Brodmann" and add "Region 6" and "Region 7." In the region window, set the "Region 6" type to "seed" and the "Region 7" type to "region-of-inclusions" (ROI).
 1. Select "New Region" in the region window and manually draw an ROI in the most posterior aspect of the superior frontal gyrus in the coronal plane. Perform fiber tracking as described in step 4.4.
 2. Place seeds for SLF II in similar fashion by using "New Region" in the region window and drawing the "seed" region in the posterior aspect of the middle frontal gyrus white matter in the coronal plane. Choose an ROI using "Atlas" (as in step 4.3.1) and Brodmann regions 9, 10, 46, 39, and 19. Perform fiber tracking as described in step 4.4.
 3. Place seeds for SLF III with a "seed" region, using "Atlas" (as in step 4.3.1) in the region window and choosing "Region 40" of the Brodmann atlas and the ROI from "Atlas..." in "Region 40" and "Region 44." Perform fiber tracking as described in step 4.4.
 4. Place seeds for callosal fibers using "New Region" in the region window and drawing a "seed" in the sagittal plane encompassing the corpus callosum. Perform fiber tracking as described in step 4.4.
 5. Place seeds for cingulate fibers using "New Region" in the region window and drawing a "seed" region in the mid-cingulate gyrus on the coronal view. Use "New Region" to draw two ROIs, one in the more anterior cingulate and one in the posterior cingulate gyrus under coronal view. Perform fiber tracking as described in step 4.4.
 6. Place seeds for claustrorocortical fibers using "New Region" in the region window and drawing a "seed" in the claustrum with an ROI in the corona radiata using the "Atlas..." function. Select the atlas as "JHU-WhiteMatter-labels-1mm."
 1. Select and add the "Anterior_corona_radiata," "Posterior_corona_radiata," and "Superior_corona_radiata". Draw a region-of-avoidance for all fibers passing through a plane inferior to the level of the claustrum in the axial plane using "New Region" in the region window. Perform fiber tracking as described in step 4.4.
 7. Place seeds for the corticospinal tract using a "seed" from the "Atlas..." function in the region window; select "JHU-WhiteMatter-labels-1mm" and add the "Corticospinal_tract" region. Perform fiber tracking as described in step 4.4.
 8. Place seeds for the frontal aslant tract (FAT) using a "seed" region from the "Atlas..." function in the region window and selecting the Brodmann atlas and "Region 6" ROIs in "Region 44" and "Region 45." Perform fiber tracking as described in step 4.4.
 9. Place seeds for the frontostriatal tract (FST) with a "seed" in "Region 6" using the "Atlas..." function. Insert new regions in the "caudate," "putamen," and "globus pallidus" from the "HarvardOxfordSub" atlas and set the type in the region window to "end." NOTE: Fiber tracking for FST will be performed by selecting the Region 6 seed and only one of the subcortical seeds per tracking session (*i.e.*, region 6 and the caudate, followed by region 6 and the putamen, and lastly region 6 and the globus pallidus).
 1. Perform fiber tracking as described in step 4.4 for each combination.
4. **Perform fiber tracking for each of the above combinations.**
 1. In the "Options" window, set the tracking parameters as: termination index of qa of 0.08, angular threshold of 75, step size of 0.675, smoothing of 0.2, minimum length of 20 mm, and maximum length of 200 mm. Select the seed orientation as "All," the seed position as "Subvoxel," and randomize seeding as "On." Use trilinear direction interpolation with a streamline (Euler) tracking algorithm. For each combination of regions above, choose "Run tracking" in the "Fiber Tracts" window. NOTE: Due to the randomized nature of the tracking, clear "false fibers" are identified and selectively removed, with regions-of-avoidance drawn by hand as a "New Region."
5. Affine register the brain-extracted T1-weighted 3D MP-RAGE scan provided in the Human Connectome Project data set to the diffusion data using the "Slices -> Insert T1/T2 Images" function of DSI-Studio. Generate a surface rendering of the brain by selecting "Slices -> Add Isosurface." Use a "threshold" of 665.

Representative Results

The SMA complex is situated in the posterior part of the superior frontal gyrus. The borders of the SMA complex are the precentral sulcus posteriorly, the superior frontal sulcus inferior-laterally, and the cingulate sulcus inferior-medially¹⁸. The SMA complex consists of two parts: the pre-SMA anteriorly and the SMA proper posteriorly¹⁸. There are differences in terms of white matter connections and function between these two parts¹⁸ (**Figure 1A** and **B**). We studied cortical and subcortical connections of these two parts using fiber dissection and DTI techniques and showed them in 3D images.

Association Fibers of the SMA Complex

Removing the cortex of the frontal lobe exposed the short association fibers, the so-called U-fibers, which interconnect neighboring gyri¹⁸ (**Figure 1C**). The short association fibers of the SMA complex provide connections between the SMA complex and the motor cortex posteriorly and between the SMA complex and the pre-frontal cortex anteriorly¹⁸ (**Figure 2B**). They also provide connections between the pre-SMA and the SMA proper in the SMA complex. The most superficial long association fibers are the superior longitudinal fasciculus II (SLF II) and the frontal opercular part of the SLF III^{13,36} (**Figure 2A**). We removed the SLF II and SLF III just in front of the precentral sulcus to expose the frontal aslant tract (FAT), which interconnects the superior frontal gyrus and the inferior frontal gyrus (**Figure 2B**). The FAT are superficial association fibers that arise from the pre-SMA and the pars opercularis.

During FAT dissection, it is critical to anatomically distinguish the FAT from corona radiata fibers, which run parallel in the vertical plane. As the literature indicates, FAT fibers travel obliquely from the SMA region to the inferior frontal gyri and become superficial in pars opercularis². However, other corona radiata and claustrorocortical fibers run deeply to the basal ganglia without being superficial¹⁸ (**Figure 2C**, **3C**, and **3D**).

Another association fiber tract of the SMA complex is SLF I, which connects the superior parietal lobe to the superior frontal lobe (SMA complex) and the anterior cingulate cortex on the medial side of the hemisphere^{18,36}. The dissection of SLF I was performed medial to lateral after the decortication of the medial surface of the hemisphere (**Figure 2A**, **3A**, and **3B**).

Commissural Fibers of the SMA Complex

The major commissural fiber pathway is the callosal fibers, which connect the SMA complex with the contralateral SMA complex. The callosal fibers are positioned between the corona radiata, the cingulum, and SLF I fibers and cross to the midline via the corpus callosum to reach the contralateral SMA complex (**Figure 2A**, **4A**, and **4B**).

Projection Fibers of the SMA Complex

The projection fibers consist of 4 different fiber groups related to the SMA complex: the cingulum fibers, claustrorocortical fibers, frontocitriatal tract, and corticospinal tract. The cingulum fibers originate from the medial surface of the hemisphere to form the cingulum and run within the cingulate gyrus. The function of these fibers is to provide connections between the SMA complex and the limbic system¹⁸ (**Figure 2A** and **4C**).

The distribution of the claustrorocortical fibers borders are the anterior edge of the pre-SMA anteriorly and the posterior part of parietal lobe posteriorly (**Figure 2D** and **4D**). Therefore, the fibers originating from the claustrum terminate in all SMA complex areas (pre-SMA and SMA proper)³⁷.

The frontostriatal tract (FST) connects the SMA complex and the dorsal striatum (*i.e.*, caudate nucleus and putamen) and travels between the external and internal capsules¹⁸ (**Figure 3C** and **3D**). It is difficult to distinguish the FST from other internal capsule fibers (*e.g.*, the thalamic peduncles, frontopontine fibers, etc.), as well as from other fibers in the vertical plane (*e.g.*, FAT and other corona radiata fibers), when using the fiber dissection technique. Nevertheless, Grande *et al.* used the DTI technique to demonstrate that the FST fibers that arise from the SMA complex terminate in both the external and internal capsules¹⁸. Approximately 10% of the cortical spinal tract fibers arise from the SMA proper and terminate in the spinal cord, but these fibers do not arise from the pre-SMA³⁸ (**Figure 4E**).

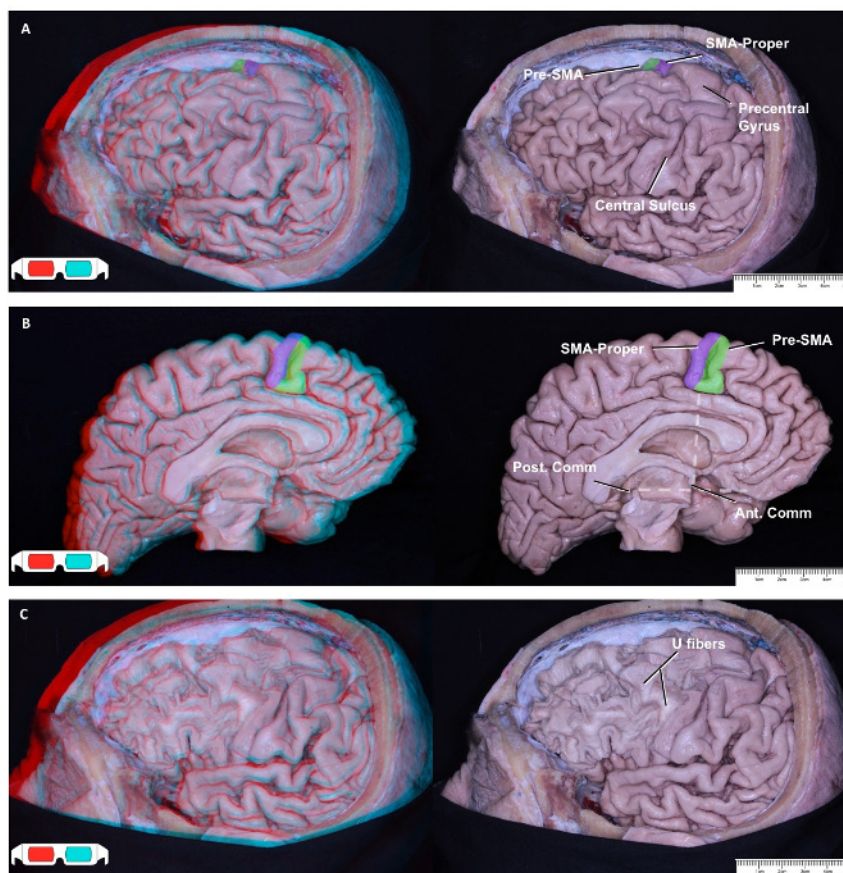


Figure 1: Lateral and Medial Surface of Left Frontal Lobe View. Labeled 2D illustrations accompany each 3D illustration on the left side. Left hemisphere lateral view: SMA proper (purple) and pre-SMA (green); the SMA complex is situated in the posterior part of the superior frontal gyrus, just in front of the precentral gyrus (A). Left hemisphere medial view. An imaginary vertical line at the level of the anterior commissure, perpendicular to the line that lies between the anterior and posterior commissures, is the border between the SMA proper (purple) and the pre-SMA (green) (B)³⁹. After decortication view. The decortication exposes short association fibers, called "U fibers." U fibers connect neighboring gyri to each other, such as the pre-SMA to the SMA proper and the SMA proper to the motor cortex (C). [Please click here to view a larger version of this figure.](#)

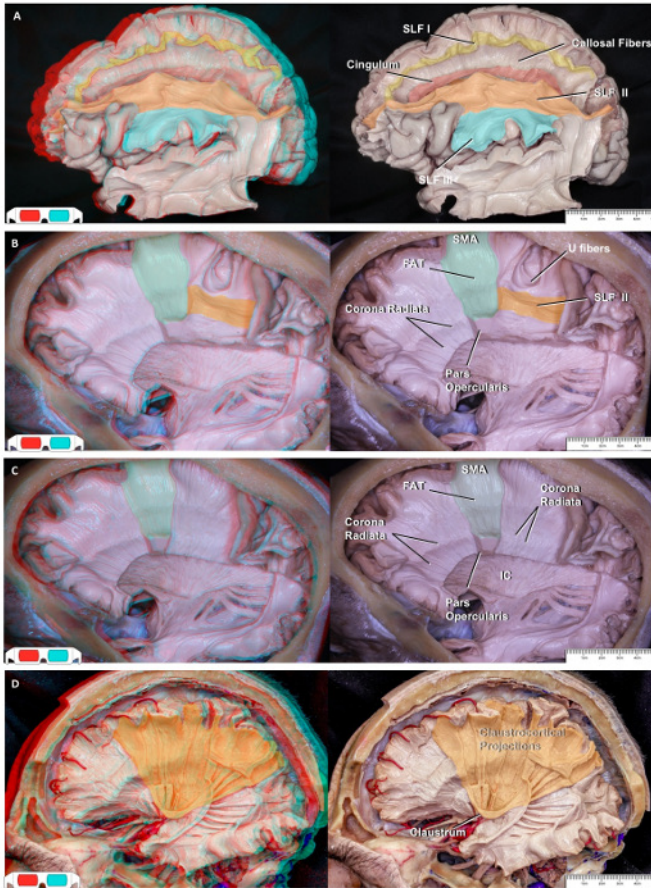


Figure 2: Lateral-to-medial Fiber Dissection. Labeled 2D illustrations accompany each 3D illustration on the left side. Lateral view; the SLF II extends between the angular gyrus and the middle frontal gyrus and terminates at the pars opercularis and pars triangularis. The SLF III connects the supramarginal gyrus and the pars triangularis in the frontoparietal operculum. Medial view; the SLF I connects the superior parietal lobe to the anterior cingulate cortex and the medial surface of the superior frontal gyrus, which includes the SMA complex (A). After removing a part of SLF II at the coronal level, the FAT was exposed (B). FAT fibers travel obliquely from the SMA region to the inferior frontal gyri and become superficial in the pars opercularis. Other corona radiata fibers run deep to the basal ganglia without being superficial (C). Another specimen showing the exposed borderline of the claustroradial fiber distribution on the cortical area, which is between the anterior part of the pre-SMA and the posterior part of the parietal lobe (D). [Please click here to view a larger version of this figure.](#)

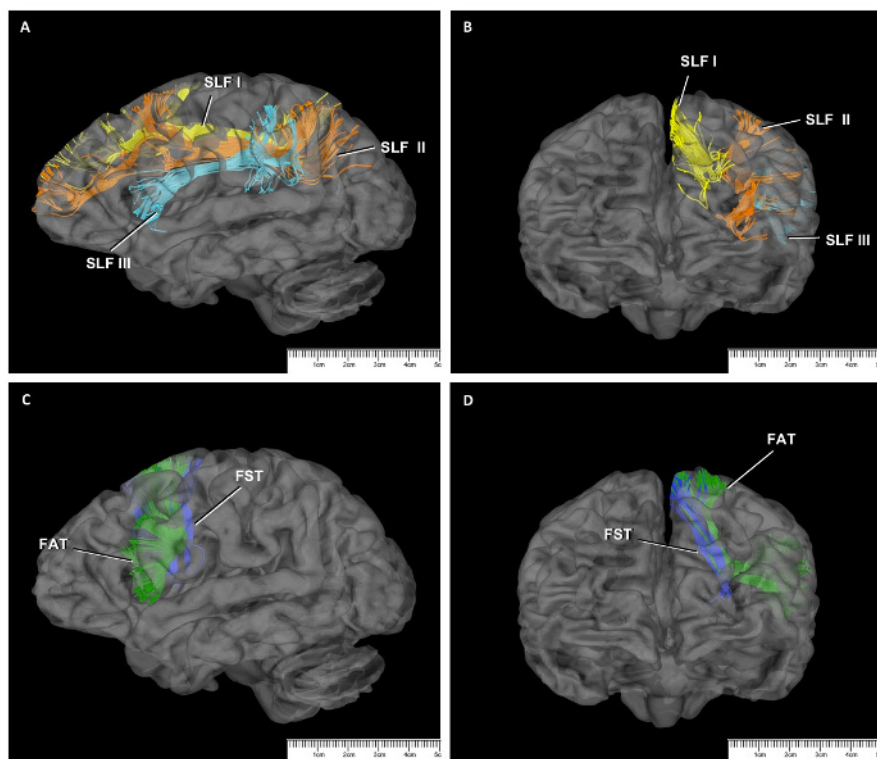


Figure 3: DTI Study of SMA Connections. SLF fibers seen on a sagittal slice (A) and a coronal slice (B) on DTI. SLF I (yellow); SLF II (orange); SLF III (turquoise). Relationship of FAT (green) and FST (blue) sagittal (C) and coronal (D) slices on DTI. [Please click here to view a larger version of this figure.](#)

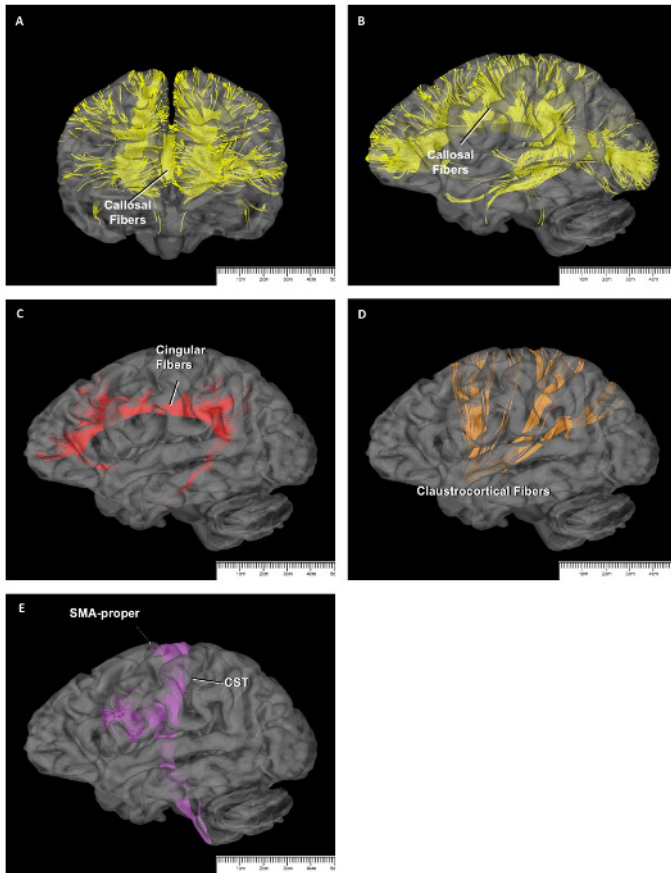


Figure 4: DTI Study of SMA Connections. Callosal fibers seen on a coronal slice (A) and a sagittal slice (B) on DTI. The cingular fibers (red) (C), the claustrorotational fibers (orange) (D), and the corticospinal tract (purple) (E), as seen on sagittal slices on DTI. [Please click here to view a larger version of this figure.](#)

Discussion

The Importance of and Study Techniques for the White Matter Pathways

The cerebral cortex is accepted as a principal neural structure associated with 2.5 million years of human life. Approximately 20 billion neurons have separated into various parts based upon morphological and cellular specification⁴⁰. The architecture of each of these cortical parts has been functionally sub-grouped, such as sensorimotor sense and movement, emotional experience, and complex reasoning. It was determined that all behaviors in primates have been formed by unique anatomo-functional connections and regions topographically distributed through the cortical and subcortical areas of the neural system. Although the cerebral cortex has been researched in detail, there is still a lack of knowledge on the white matter pathways of the neural system that connect different areas. Areas such as the centrum semiovale and corona radiata have been studied before under a macroscopic view. During the 1800s, researchers performed the gross dissection of monkeys using myelin coloring materials and autoradiography methods that were applied with the help of amino acids to understand the white matter fiber system. Some major association fibers, such as the cingulum and uncinate fasciculus, have been identified and named with these studies. On the other hand, the identification of other white matter pathways, such as the arcuate fasciculus/superior longitudinal fasciculus and the inferior longitudinal fasciculus, is still contradictory in the literature^{41,42,43,44,45}.

An understanding of white matter structures is very important to providing details on the anatomical processes of high-level behavior and the structure and function of the cerebrum. A deeper understanding of the white matter pathways is also critical for clinical aims. Many diseases are caused by lesions affecting the white matter pathways. Previously, there was no unique and proper technique that could be used to describe the fiber pathways, despite improvements in radiological imaging techniques. The cadaveric fiber dissection technique, which is the oldest technique, was the ideal method for the neuroanatomical education of young neurosurgeons and the best standard among the tractography techniques based upon diffusion tensor imaging, MR tractography, diffusion spectrum tractography, and autoradiography. The fiber tracts can be visualized *in vivo* with MRI; however, the disadvantage of this technique is the difficulty in determining the termination and the origin of the fiber pathways. The autoradiographic technique can only be used in experimental animals. A knowledge of fiber tract anatomy is critical to gaining a better understanding of cognitive, psychiatric, and motor manifestations following white matter disorders such as multiple sclerosis.

Plasticity exists in gray matter, but not in white matter; any peri-operative damage to white matter causes irreversible deficits in the patient (Schmahmann *et al.*). This renders the anatomy of the fiber pathways more valuable in neurosurgery⁴⁶. During preoperative surgical planning for the removal of intra-axial lesions, the location and displacement of the important fiber pathways, such as the arcuate fasciculus, optic radiations, and corticospinal tract should be taken into consideration for a successful surgery. The anatomical knowledge, together with preoperative MR

tractography, provide sound evaluation and surgical planning for each patient. In the meantime, performing cadaveric fiber dissection under the operating microscope helps to improve the hand skills of the surgeon and provides a deeper understanding of the complex brain anatomy in three dimensions. To achieve these gains, the surgeon should spend time in a microsurgery laboratory. He/she should only focus on the fiber tracts during the dissection, rather than what he/she would like to see. On the other hand, today, improvements in DTI imaging techniques have made it possible to identify major fiber pathways *in vivo*, both in the normal brain and in clinical situations where the fiber system is affected. Initially, this method did not provide any information about the start and termination regions of major fiber bundles and was only effective in the definition of extensions. However, with the development of MR tractography and diffusion spectrum imaging (DSI), major steps have been taken to understand normal brain anatomy in *in vivo* and clinical studies^{47,48,49}. In recent years, it has been suggested that mapping of white matter pathways is very critical to prevent postoperative deficits. It is also useful to perform intraoperative electrical mapping of the white matter to help protect significant subcortical structures and their functions^{50,51}. Therefore, the anatomy of the frontal region and the white matter pathways should be understood thoroughly for frontal-glioma surgery.

Anatomic Features and the Clinical Importance of SMA Complex

The macro-anatomical border line between the pre-SMA and the SMA proper is accepted as a vertical imaginary line passing through the level of the anterior commissure^{18,39}. Also, the pre-SMA and the SMA proper have differences in terms of their functions. Although the SMA proper has somatotopic tasks, the pre-SMA has a somatosensory organization¹⁹. Basically, the SMA proper is responsible for the activation, control, and generation of movement, while the pre-SMA is responsible for cognitive and non-motor tasks⁸.

Patients with lesions of the pre-SMA present with various degrees of speech impairment, ranging from a total inability to initiate speech (*i.e.*, mutism) to mild altered fluency⁵². As would be predicted by neurosurgical electrical stimulation data, resection or damage to the SMA complex produces negative motor response in motor and speech functions and eventually results in SMA syndrome. SMA syndrome is a complex neurosurgical syndrome of initiation that ranges from a total loss of motor and speech production, such as akinetic mutism, to diminished spontaneous movements and speech^{18,53}. Therefore, the subcortical fiber tract connections of the SMA complex play an important role in surgical planning.

The Fiber Tracts of the SMA Complex

In this study, we studied all connections of the SMA complex, such as the FAT, FST, short association fibers, SLF I, callosal fibers, cingulum fibers, and claustricofrontal fibers using cadaveric fiber dissection and DTI techniques that were defined in the literature in recent years^{8,13,18}. We showed and supported our fiber dissection results via DTI. However, it is difficult to separate some projection white matter pathways, such as the FST and the corticospinal tract (CST) from other corona radiata fiber bundles via anatomical dissection. Therefore, we were able to show the topographical anatomy of these two fiber bundles more effectively via DTI. Additionally, the ability to study *in vitro* and to display deep fiber bundles in detail are the other advantages of DTI study.

The SLF I is a long association fiber that which connects the precuneus (superior parietal lobe) to the SMA complex and cingulate cortex. SLF I has functions relating to both the limbic system, by connecting with the anterior cingulate cortex, and the motor system, by connecting with the superior parietal lobe^{13,18,36,54}.

The posterior parts of the superior and inferior frontal gyrus interconnect with a direct system that consist of the FAT, which was newly defined using DTI techniques² and then with fiber dissection techniques¹⁸. The projection of this pathway is in the pre-SMA and SMA proper in the superior frontal gyrus and the pars opercularis in the inferior frontal gyrus¹⁸. Ford *et al.* demonstrated structural connectivity between the SMA and the Broca center for the first time, supporting the functional role of the SMA as a speech-processing cortex⁵⁵. In addition to the SLF I, the FAT is a direct pathway connecting the pars opercularis with the anterior cingulate and pre-SMA, as indicated by the results in this study. Catani *et al.* defined the FAT through DTI and reported that cortical atrophy of the FAT connection zones on the SMA complex (pre-SMA and anterior part of the SMA proper) and the anterior cingulate in patients with primary progressive aphasia may result in verbal fluency disorders⁴⁶. Previous studies have indicated that FAT may also be associated with speech initiation difficulties and speech fluency dysfunctions²².

The FST is made up of projection fibers that connect the pre-SMA and striatum (*i.e.*, caudate nucleus and putamen). In previous studies, the termination points of the FST in the basal ganglia were not very clear. However, it was also shown in recent comprehensive DTI studies that the FST originates from the pre-SMA and terminates in the internal capsule and in the lateral surface of the putamen^{20,21,22}. In addition to this, in another DTI study, it has been shown that the FST terminates both in the lateral and the medial surfaces of the putamen¹⁸. Functionally, Duffau *et al.* demonstrated anarthria and/or cessation of movement during intraoperative direct electrical stimulation of the putamen, the mechanism of which is most likely through the putaminal connections of the FST²¹.

The corticospinal tract connects the SMA proper and primary motor cortex to the spinal cord, but the pre-SMA has no fibers of the corticospinal tract²⁴. In an electrostimulation study by Duffau *et al.*, an arrest of movement was observed by stimulating the SMA region in the contralateral upper limb. It was thought that this may occur because of the connection of the SMA with the spinal cord by the corticospinal tract and the contralateral SMA by callosal fibers^{18,56}.

The claustricofrontal fibers connect between the claustrum in the central core and a wide region between the anterior edge of the pre-SMA and the posterior part of the parietal lobe¹³. Functionally, the claustricofrontal fibers are believed to play a role in consciousness and in coordinating information coming from the visual cortical region, limbic system, and somatosensory and motor cortices²⁷. Therefore, claustricofrontal fiber bundles between the SMA complex and the claustrum were thought to may play a role in the execution of higher motor and speech control¹⁸.

Although has been stated in previous studies that the connection of SMA complex with cingular gyrus is via short association fibers, in a recent anatomical study, it was found that these connections are provided directly by cingular fibers¹⁸. Functionally, it was claimed that this pathway has a role in the motor processing of negative emotional stimulation between the SMA and the limbic cortex¹⁸.

In recent years, the clinical importance of the SMA complex (*e.g.*, SMA syndrome and negative motor response) was revealed by an increasing number of electrostimulation studies. Therefore, the importance of topographical anatomy and subcortical connections of the SMA were

gradually highlighted. It is critical to gain a better understanding of topographical anatomy, particularly through 3D anatomical studies, and to use clinical features of these connections to plan surgery.

Disclosures

The authors declare no competing financial interests and no sources of funding and support, including any for equipment and medications.

Acknowledgements

The data were provided in part by the Human Connectome Project, WU-Minn Consortium (Principal Investigators: David Van Essen and Kamil Ugurbil; 1U54MH091657), funded by the 16 NIH Institutes and Centers that support the NIH Blueprint for Neuroscience Research; and by the McDonnell Center for Systems Neuroscience at Washington University. Figures 2A and 2D were reproduced with permission from the Rhoton collection⁵⁷ (<http://rhoton.ineurodb.org/?page=21899>).

References

1. Nieuwenhuys, R., Voogd J., Huijzen, CV. *The Human Central Nervous System*. 4th ed., 620-649 (2008).
2. Catani, M., Acqua, F., Vergani, F., Malik, F., Hodge, H. Short frontal lobe connections of the human brain. *Cortex*. **48** (2) 273-91. (2012).
3. Duffau, H., Capelle, L. Preferential brain locations of low-grade gliomas. *Cancer*. **100** (12), 2622-6 (2004).
4. Yasargil, M.G., Türe, U., Yasargil, D.C. Impact of temporal lobe surgery. *J Neurosurg*. **101** (05), 725-738, (2004).
5. Türe, U., Yasargil, M. G., Friedman, A. H., & Al-Mefty, O. Fiber dissection technique: lateral aspect of the brain. *Neurosurgery*. **47**(2), 417-427, (2000).
6. Burger, P.C., Heinz, E.R., Shibata, T., Kleihues, P. Topographic anatomy and CT correlations in the untreated glioblastoma multiforme. *J Neurosurg*. **68**(5), 698-704, (1998).
7. Duffau, H. New concepts in surgery of WHO grade II gliomas: Functional brain mapping, connectionism and plasticity-a review. *J Neurooncol*. **79** (1), 77-79, (2006).
8. Vergani, F. et al. White matter connections of the supplementary motor area in humans. *J Neurol Neurosurg Psychiatry*. **85**(12), 1377-85, (2014).
9. Luppino, G., Matelli, M., Camarda, R., Rizzolatti, G. Corticocortical connections of area F3(SMA-proper) and area F6(pre-SMA) in the macaque monkey. *J. Comp.Neurol*. **338**, 114-140 (1993).
10. Akkal, D., Dum, R.P., Strick, P.L. Supplementary motor area and presupplementary motor area: targets of basal ganglia and cerebellar output. *J. Neurosci*. **27**, 10659-10673 (2007).
11. Behrens, T.E. et al. Non-invasive mapping of connections between human thalamus and cortex using diffusion imaging. *Nat. Neurosci*. **6**, 750-757 (2003).
12. Potgieser, A.R.E., de Jong, B.M., Wagemakers, M., Hoving, E.W., & Groen, R.J.M. Insights from the supplementary motor area syndrome in balancing movement initiation and inhibition. *Frontiers in Human Neuroscience*. **28** (8), 960 (2014).
13. Yagmur, K., Vlasak, A.L., & Rhoton Jr, A.L. Three-Dimensional Topographic Fiber Tract Anatomy of the Cerebrum. *Neurosurgery*. (epub), **2**, 274-305, (2015).
14. Fernández-Miranda, J. C., Rhoton Jr, A. L., Álvarez-Linera, J., Kakizawa, Y., Choi, C., & de Oliveira, E. P. Three-dimensional microsurgical and tractographic anatomy of the white matter of the human brain. *Neurosurgery*. **62**(6 Suppl 3), 989-1026 (2008).
15. Couzin, J. Crossing a frontier: Research on the dead. *Science*. **299** (5603), 29-30, (2003).
16. University of Minnesota. *Research Ethics*. [https://www.ahc.umn.edu/img/assets/26104/Research Ethics/pdf](https://www.ahc.umn.edu/img/assets/26104/Research%20Ethics.pdf). (2016).
17. Ludwig, E., Klingler, J. Der innere Bau des Gehirns dargestellt auf Grund makroskopischer Präparate. The inner structure of the brain demonstrated on the basis of macroscopical preparations. *Atlas cerebri humani*. 1-36 (1956).
18. Bozkurt, B. et al. The Microsurgical and Tractographic Anatomy of the Supplementary Motor Area Complex in Human. *J World Neurosurg*. **95**, 99-107 (2016).
19. Lehericy, S. et al. 3-D diffusion tensor axonal tracking shows distinct SMA and pre-SMA projections to the human striatum. *Cereb Cortex*. **14**, 1302-1309, (2004).
20. Duffau, H. et al. Intraoperative mapping of the cortical areas involved in multiplication and subtraction: an electrostimulation study in a patient with a left parietal glioma. *J Neurol Neurosurg Psychiatry*. **73**(6), 733-738, (2002).
21. Kinoshita, M. et al. Role of fronto-striatal tract and frontal aslant tract in movement and speech: an axonal mapping study. *Brain Struct Funct*. **220**(6), 3399-3412 (2015).
22. Shimizu, S. et al. Anatomic dissection and classic three-dimensional documentation: a unit of education for neurosurgical anatomy revisited. *Neurosurgery*. **58**(5), E1000, (2006).
23. Connectome Database. <https://db.humanconnectome.org>. (2016).
24. Moeller, S. et al. Multiband multislice GE-EPI at 7 tesla, with 16-fold acceleration using partial parallel imaging with application to high spatial and temporal whole-brain fMRI. *Magn Reson Med*. **63**(5), 1144-1153 (2010).
25. Feinberg, D.A. et al. Multiplexed Echo Planar Imaging for sub-second whole brain fMRI and fast diffusion imaging. *PLoS One*. **5**, e15710, (2010).
26. Setsompop, K. et al. Blipped-controlled aliasing in parallel imaging for simultaneous multislice echo planar imaging with reduced g-factor penalty. *Magn Reson Med*. **67**(5), 1210-1224, (2012).
27. Xu, J. et al. Highly accelerated whole brain imaging using aligned-blipped-controlled-aliasing multiband EPI. In *Proceedings of the 20th Annual Meeting of ISMRM*. **20**, 2306, (2012).
28. Glasser, M.F. et al. The minimal preprocessing pipelines for the Human Connectome Project. *Neuroimage*. **80**, 105-124, (2013).
29. Free Surfer software suite. Harvard University. <http://surfer.nmr.mgh.harvard.edu>. (2016).
30. FSL. Software Library. <http://fsl.fmrib.ox.ac.uk>. (2016).

31. Jenkinson, M., Bannister, P.R., Brady, J.M., and Smith, S.M. Improved optimization for the robust and accurate linear registration and motion correction of brain images. *NeuroImage*. **17**(2), 825-841, (2002).
32. Andersson, J.L., Skare, S., and Ashburner, J. How to correct susceptibility distortions in spin-echo echo-planar images: application to diffusion tensor imaging. *NeuroImage*. **20**(2), 870-888, (2003).
33. Andersson, J., Xu, J., Yacoub, E., Auerbach, E., Moeller, S., and Ugurbil, K. A comprehensive Gaussian process framework for correcting distortions and movements in diffusion images. *In Proceedings of the 20th Annual Meeting of ISMRM*. **20**, 2426, (2012).
34. DSI Studio. <http://dsi-studio.labsolver.org> (2016).
35. Yeh, F.C., Wedeen, V.J., Tseng, W.Y. Generalized q-sampling imaging. *IEEE Trans Med Imaging*. **29**(9), 1626-35 (2010).
36. Makris, N. *et al.* Segmentation of subcomponents within the superior longitudinal fascicle in humans: a quantitative, in vivo, DT-MRI study. *Cereb Cortex*. **15**(6), 854-869 (2005).
37. Fernández-Miranda, J.C., Rhoton, A.L. Jr, Kakizawa, Y., Choi, C., Alvarez-Linera, J. The claustrum and its projection system in the human brain: a microsurgical and tractographic anatomical study. *J Neurosurg*. **108**(4), 764-774 (2008).
38. Maier, M.A., Armand, J., Kirkwood, P.A., Yang, H.W., Davis, J.N., and Lemon, R. N. Differences in the corticospinal projection from primary motor cortex and supplementary motor area to macaque upper limb motoneurons: an anatomical and electrophysiological study. *Cereb. Cortex*. **12**, 281-296 (2002).
39. Picard, N., Strick, P.L. Imaging the premotor areas. *Curr. Opin. Neurobiol*. **11**, 663-672, (2001).
40. Pakkenberg, B., & Gundersen, H. J. G. (1997). Neocortical neuron number in humans: effect of sex and age. *Journal of Comparative Neurology*. **384**(2), 312-320 (1997).
41. Geschwind, N. Disconnexion syndromes in animals and man. *Brain*. **88**(3), 237-294 (1965).
42. Geschwind, N. Disconnexion syndromes in animals and man. *Brain*. **88**(3), 585-644 (1965).
43. Goldman-Rakic, P. S. Topography of cognition: parallel distributed networks in primate association cortex. *Annu Rev Neurosci*. **11**(1), 137-156 (1988).
44. Mesulam, M. M. From sensation to cognition. *Brain*. **121**(6), 1013-1052, (1998).
45. Mesulam, M. Large-scale neurocognitive networks and distributed processing for attention, language, and memory. *Ann Neurol*. **28**(5), 597-613, (1990).
46. Schmahmann, J.D., Pandya, D.N. Fiber pathways of the brain. Oxford: *Oxford University Press*. **8**, 393-409, (2006).
47. Bammer, R., Acar, B., & Moseley, M. E. In vivo MR tractography using diffusion imaging. *Eur J Radiol*. **45**(3), 223-234, (2003).
48. Catani, M., Howard, R. J., Pajevic, S., & Jones, D. K. Virtual in vivo interactive dissection of white matter fasciculi in the human brain. *Neuroimage*. **17** (1), 77-94, (2002).
49. Lin, C. P., Wedeen, V. J., Chen, J. H., Yao, C., & Tseng, W. Y. I. (2003). Validation of diffusion spectrum magnetic resonance imaging with manganese-enhanced rat optic tracts and ex vivo phantoms. *Neuroimage*. **19**(3), 482-495, (2003).
50. Bello, L., Acerbi, F., Giussani, C., Baratta, P., Taccone, P., & Songa, V. Intraoperative language localization in multilingual patients with gliomas. *Neurosurgery*. **59**(1), 115-125, (2006).
51. Bernstein, M. Subcortical stimulation mapping. *J Neurosurg*. **100**(3), 365, (2004).
52. Ackermann, H., Riecker, A. The contribution(s) of the insula to speech production: a review of the clinical and functional imaging literature. *Brain Struct Funct*. **214**, 419-433 (2010).
53. Krainik, A. *et al.* Role of the healthy hemisphere in recovery after resection of the supplementary motor area. *Neurology*. **62**, 1323-1332, (2004).
54. Ford, A., McGregor, K.M., Case, K., Crosson, B., White, K.D. Structural connectivity of Broca's area and medial frontal cortex. *Neuroimage*. **52**, 1230-1237, (2010).
55. Catani, M., Mesulam, M.M., Jakobsen, E., Malik, F., Martersteck, A., Wieneke, C., Thompson, C.K. Thiebaut de Schotten M., Dell'Acqua, F., Weintraub, S., Rogalski, E. A novel frontal pathway underlies verbal fluency in primary progressive aphasia. *Brain*. **136**, 2619-2628, (2013).
56. Rech, F., Herbet, G., Moritz-Gasser, S., Duffau, H. Disruption of bimanual movement by unilateral subcortical electrostimulation. *Human Brain Mapping Annual Meeting*. **35**(7), 3439-3445 (2014).
57. The Rhoton Collection. Login page. <http://rhoton.ineurodb.org/?page=21899>. (2016).